Supporting Information

Vertically Antioxidant Strategy for High Performance Wide Band Gap Tin Perovskite Photovoltaics

Fan Hu [a], Chun-Hao Chen [a], Yan-Hui Lou [b,*], Tian-Yu Teng [a], Yi-Ran Shi [a], Yu Xia [a], Kai-Li Wang [a], Jing Chen [a], Zhao-Kui Wang [a,*], and Liang-Sheng Liao [a]

[a] *Institute of Functional Nano & Soft Materials (FUNSOM), Laboratory of Advanced Negative Carbon Technologies, Soochow University, Suzhou, Soochow University, Suzhou, Jiangsu 215123, China*

[b] *College of Energy, Soochow Institute for Energy and Materials Innovations, Soochow University Suzhou, Jiangsu 215006, China*

Corresponding Authors:
yhlou@suda.edu.cn; zkwang@suda.edu.cn

A

Supplementary Note 1. DFT calculation methods.

The optimization of the ground-state geometry for BP4Ac and BP2Ac molecules were performed with B3LYP functional and 6-31g(d,p) basis set using Gaussian09 package. The analysis of electrostatic potential (ESP) was performed within Multiwfn program. [1,2] The isosurface of van der Waals (vdW) surface was set as 0.001 e/bohr3. The electrostatic potential involved in the analyses was evaluated by Multiwfn based on the highly effective algorithm proposed in Ref. [3].

References

[1]   T. Lu, F. Chen, Multiwfn: a multifunctional wavefunction analyzer, J Comput Chem 33 (2012) 580-592.

[2]   T. Lu, S. Manzetti, Wavefunction and reactivity study of benzo [a] pyrene diol epoxide and its enantiomeric forms, Struct. Chem. 25 (2014) 1521-1533.

[3]   J. Zhang, T. Lu, Efficient evaluation of electrostatic potential with computerized optimized code, Phys. Chem. Chem. Phys. 23 (2021) 20323-20328.

Supplementary Note S2. Trap Density of States Analysis.

The distribution of trap density of states (*t*DOS) can be deduced from the angle frequency dependent capacitance measurement by the equation:

$$N_T E_\omega = -\frac{V_{bi} dC}{qW d\omega k_B T}\omega \quad (2)$$

where V_{bi} is the built-in potential, q is the element charge, W is the depletion width, ω is the applied angular frequency, k_B is the Boltzmann's constant, T is the temperature and C is the capacitance of the layer. In addition, voltage dependent capacitance measurement was applied to get a relationship between V_{bi} and W. Also, the applied angular frequency correlates with energy demarcation because trap states below the energy will attract or emit charges under this angular frequency. The correlation is given in the equation as follows:

$$E_\omega = k_B T ln\frac{\omega_0}{\omega} \quad (3)$$

where ω_0 is the attempt-to-escape frequency. According to these relationships, we finally reckoned the *t*DOS curves.

Supplementary Note S3. Solution Absorption Test.

To understand the inhibitory effect of these two acidic molecules on Sn2+ oxidation at their optimal concentrations, we tested their corresponding UV-vis absorption spectra at intervals in air. The different acidic molecules were dissolved in N, N-dimethylformamide (DMF) at their optimal concentrations and then added to the cuvette, followed by 50 μL of perovskite precursor solution to avoid saturation of the detector. Finally, the solution is monitored at intervals for its absorption signal. The absorbance spectrograms were measured through UV–vis spectrophotometer (PerkinElmer Lambda 750).

Supplementary Note S4. The Detailed Procedures for Some Important characterizations.

1. For the oxidation resistance of the precursor solution, fresh precursor solutions with and without different additives were prepared, and then perovskite films were prepared by these fresh precursor solution and the area ratio of Sn^{4+}/Sn^{2+} on the surface of perovskite film was analyzed by XPS. The fresh precursor solution was then placed in the glove box for two weeks, and perovskite films were prepared by aging solutions and Sn^{4+} content on the film surface was measured. Then the increment of Sn^{4+}/Sn^{2+} between two weeks before and two weeks after was observed to determine the antioxidant ability under different pH conditions.

2. For liquid-state ^1H nuclear magnetic resonance (^1H-NMR) characterization, we prepared BP2Ac-containing deuterated dimethyl sulfoxide reagent(DMSO-d6) and BP4Ac-containing deuterated dimethyl sulfoxide reagent(DMSO-d6). In addition, we verify the formation of hydrogen bonds by adding SnI_2 to a deuterated DMSO reagent containing two additives. ^1H NMR spectras were measured by utilizing the JNM-ECZ400S/L1 with a frequency of 400 MHz.

3. For Depth-profiling XPS characterization, We prepared perovskite films containing with/without different additives and placed them in the air for 20 min before testing to observe the antioxidant capacity of different films. And the depth-dependent XPS analyses were measured at the Jiangsu Jicui Photoelectric Test Center.
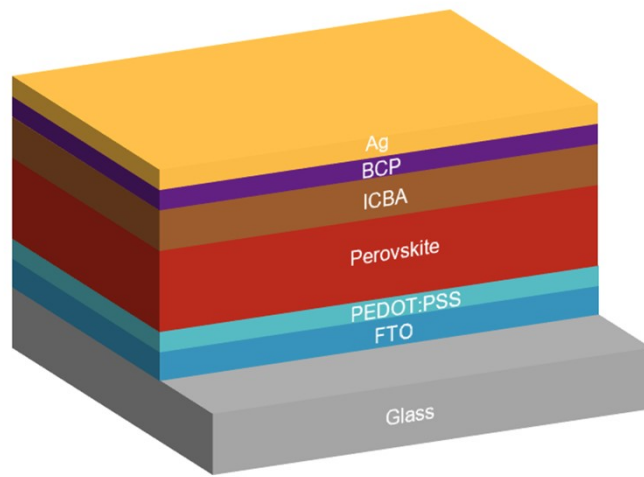
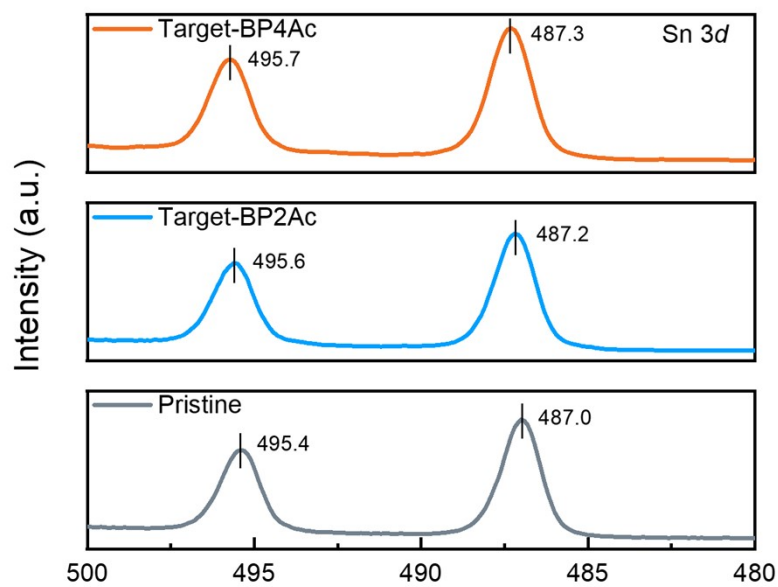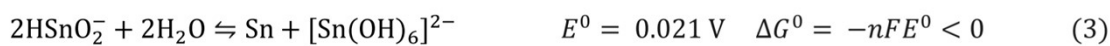**Figure S1.** Schematic illustration of inverted device structure.

Figure S2. X-ray photoelectron spectroscopy (XPS) of Sn $3d$ core levels spectra on the perovskite films.
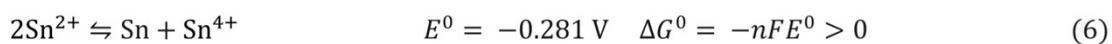
In the alkali medium:

$$HSnO_2^- + H_2O + 2e^- \leftrightharpoons Sn + 3OH^- \qquad\qquad E^0 = -0.909 \text{ V} \qquad\qquad (1)$$

$$[Sn(OH)_6]^{2-} + 2e^- \leftrightharpoons HSnO_2^- + H_2O + 3OH^- \qquad E^0 = -0.93 \text{ V} \qquad\qquad (2)$$

$$2HSnO_2^- + 2H_2O \leftrightharpoons Sn + [Sn(OH)_6]^{2-} \qquad E^0 = 0.021 \text{ V} \quad \Delta G^0 = -nFE^0 < 0 \qquad (3)$$

In the acidic medium:

$$Sn^{2+} + 2e^- \leftrightharpoons Sn \qquad\qquad\qquad\qquad E^0 = -0.13 \text{ V} \qquad\qquad (4)$$

$$Sn^{4+} + 2e^- \leftrightharpoons Sn^{2+} \qquad\qquad\qquad\qquad E^0 = 0.151 \text{ V} \qquad\qquad (5)$$

$$2Sn^{2+} \leftrightharpoons Sn + Sn^{4+} \qquad E^0 = -0.281 \text{ V} \quad \Delta G^0 = -nFE^0 > 0 \qquad (6)$$

Figure S3. The redox property of Sn^{2+} evaluated from its standard reduction potential (E^0) in the alkali or acid medium.
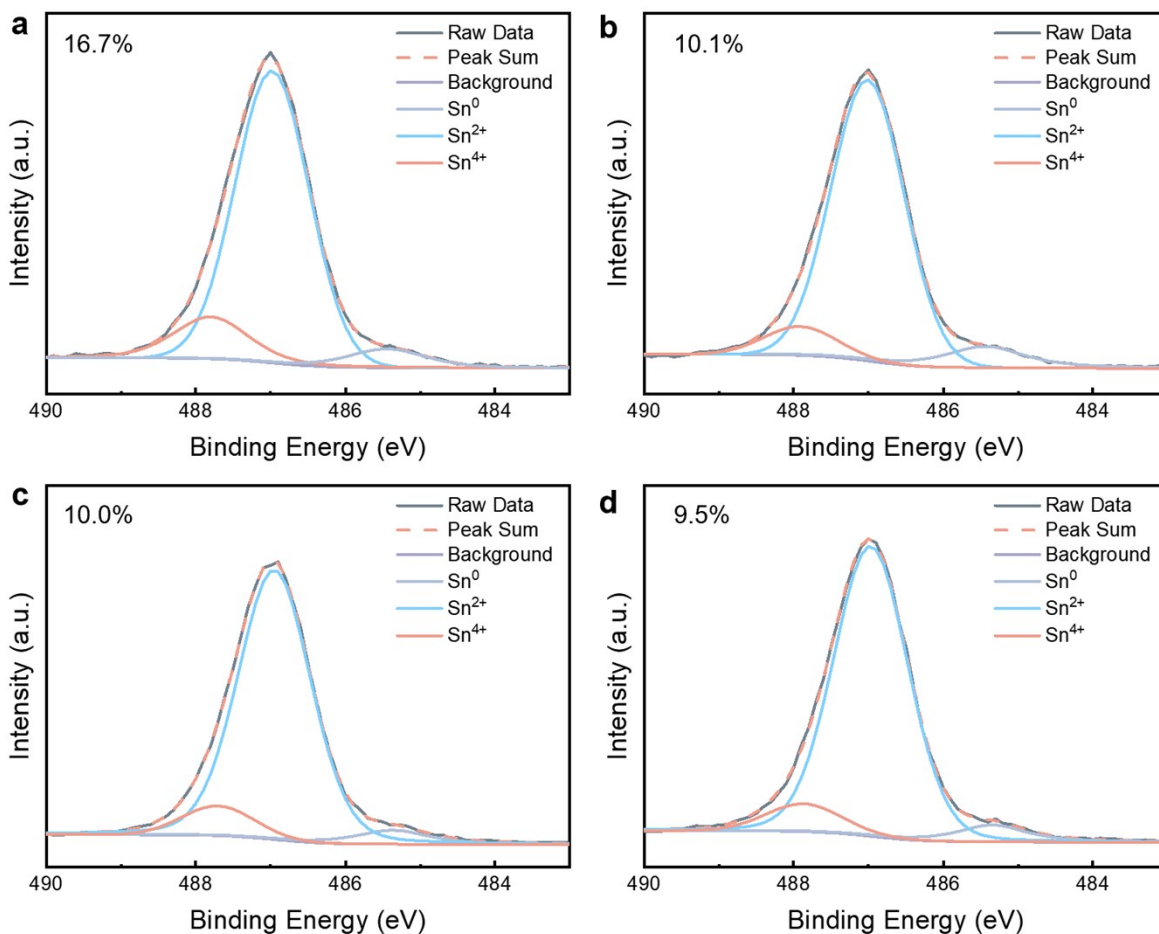
Figure S4. Sn^{2+} and Sn^{4+} signals obtained from XPS spectra of Sn $3d$ for perovskite films fabricated with fresh precursor solutions at different pH values a) pH=5.06, b) pH=4.62, c) pH=4.38 and d) pH=3.95, respectively.
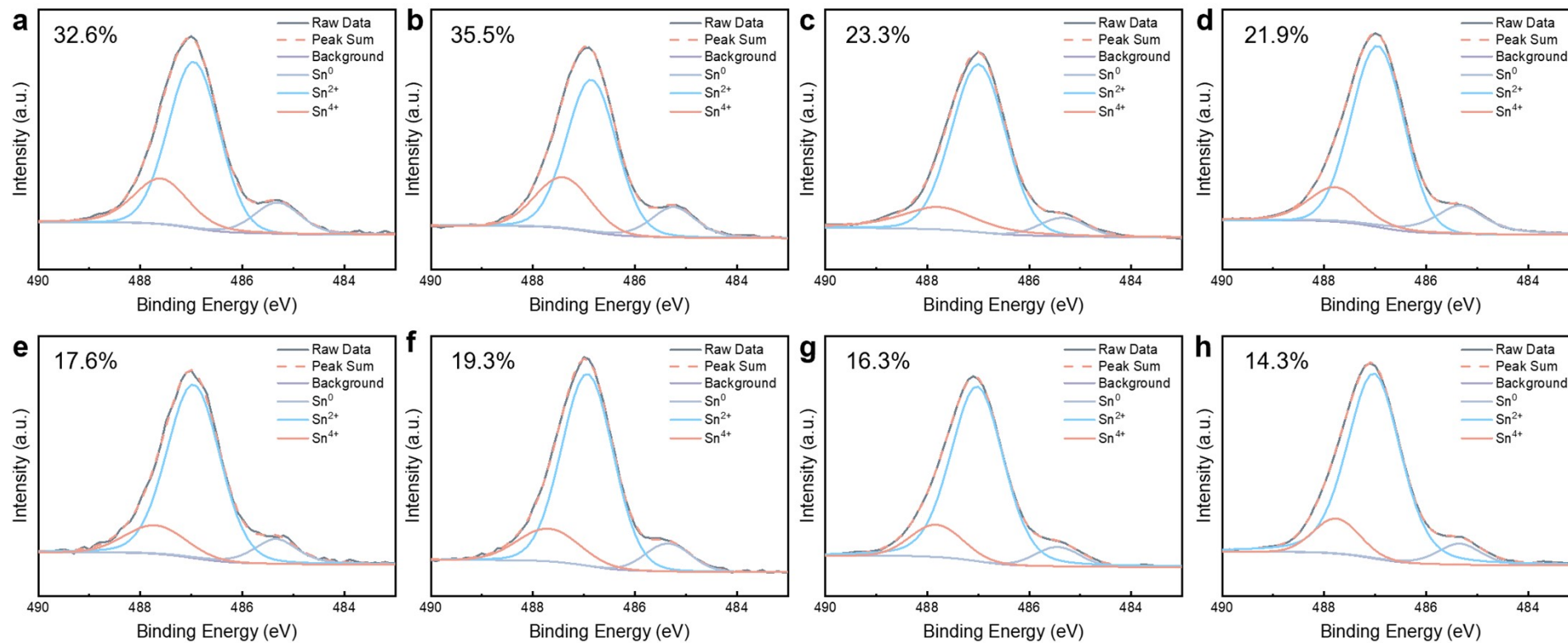
Figure S5. Sn^{2+} and Sn^{4+} signals obtained from XPS spectra of Sn $3d$ for perovskite films fabricated with precursor solutions placed in a glove box for two weeks at different pH values a,b) pH=5.06, c,d) pH=4.62, e,f) pH=4.38 and g,h) pH=3.95, respectively.
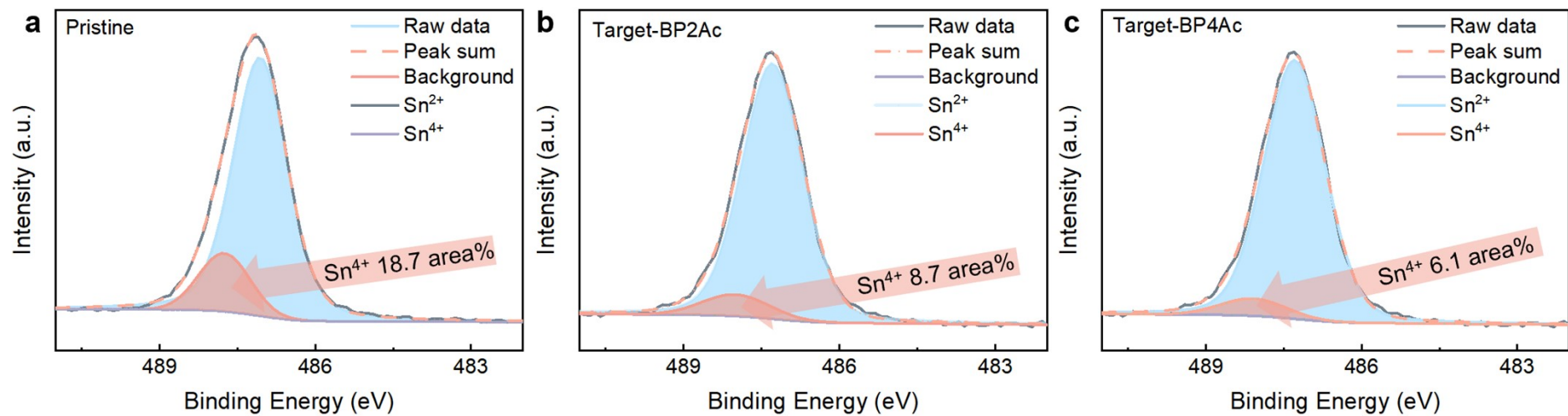
Figure S6. XPS spectra of Sn $3d$ for perovskite films w/o and with different additives.
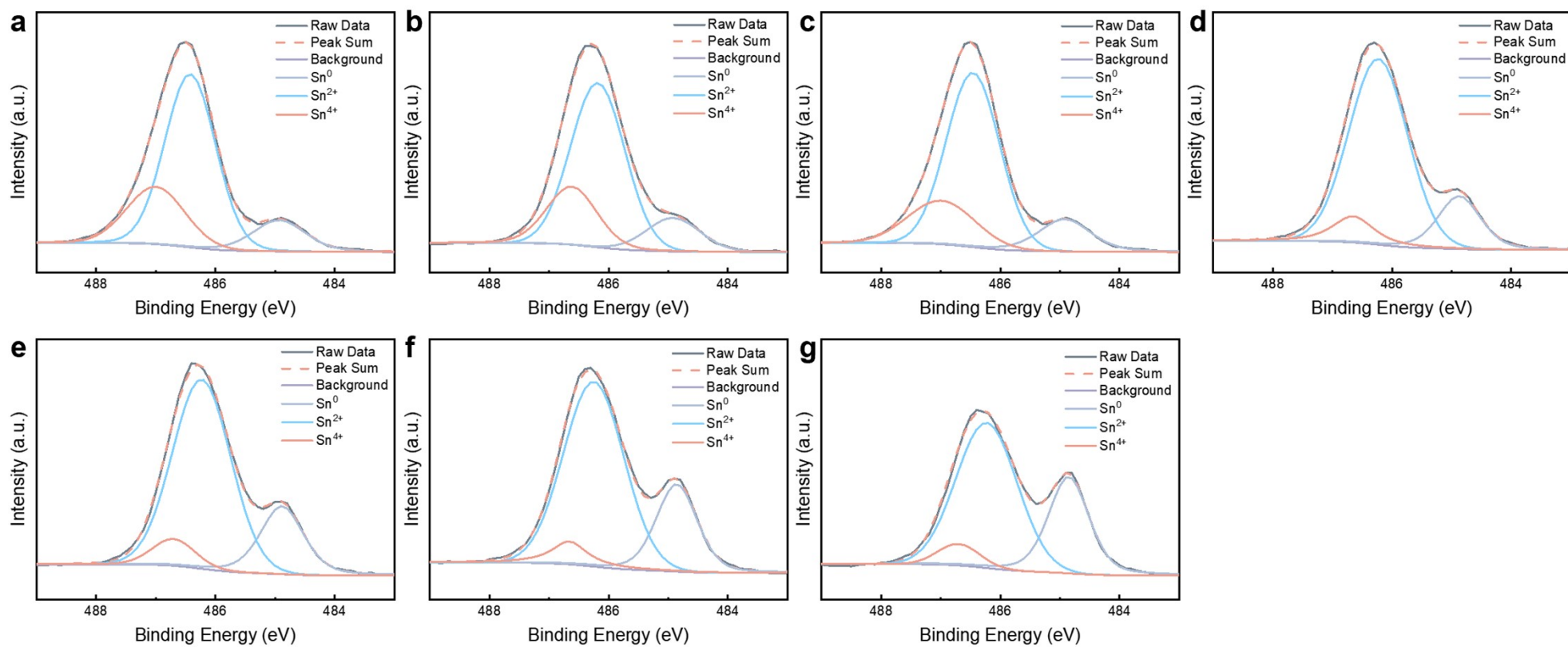
Figure S7. XPS curves of the pristine perovskite film at different etching times. From a) to g), a) is the fresh sample and b) stands for the first etching and g) represents the 6th etching result. For each etching process, the duration is 5 seconds.
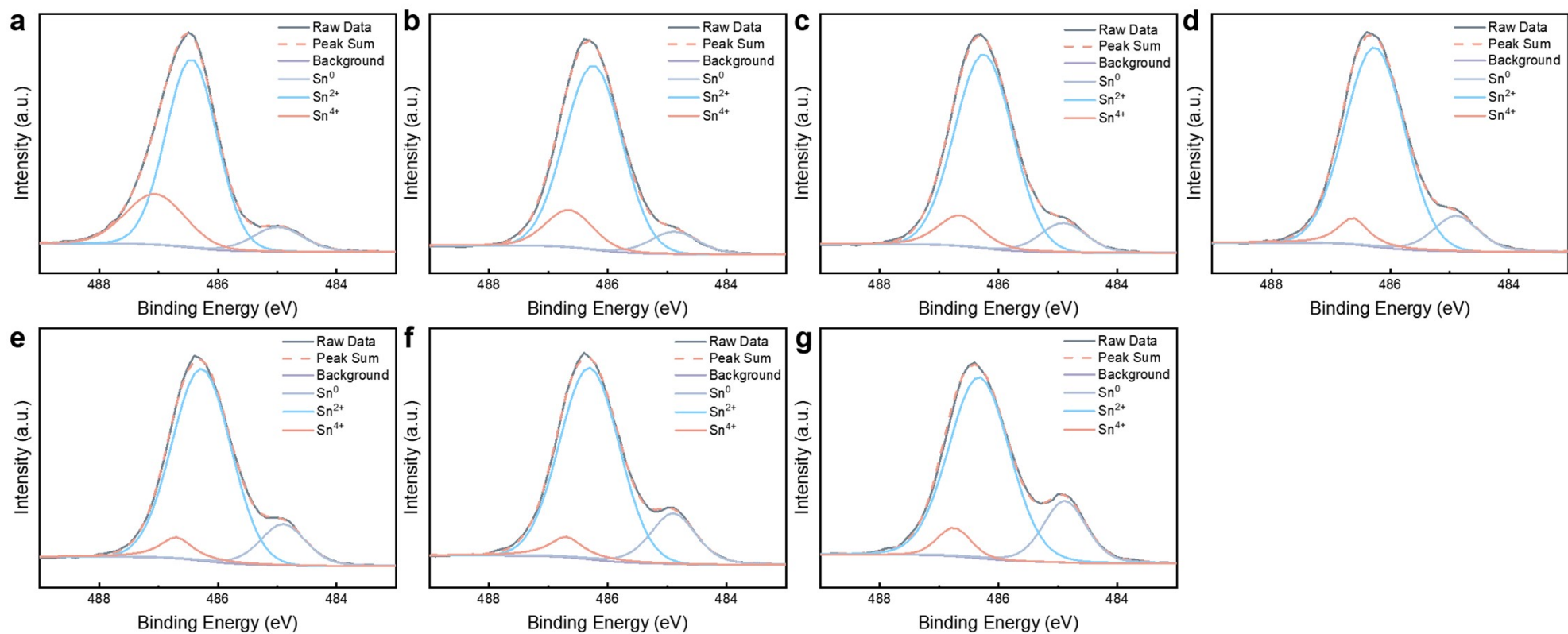
Figure S8. XPS curves of the target-BP2Ac perovskite film at different etching times. The sequence and etching time for this sample are identical with the pristine sample shown in Figure S7.
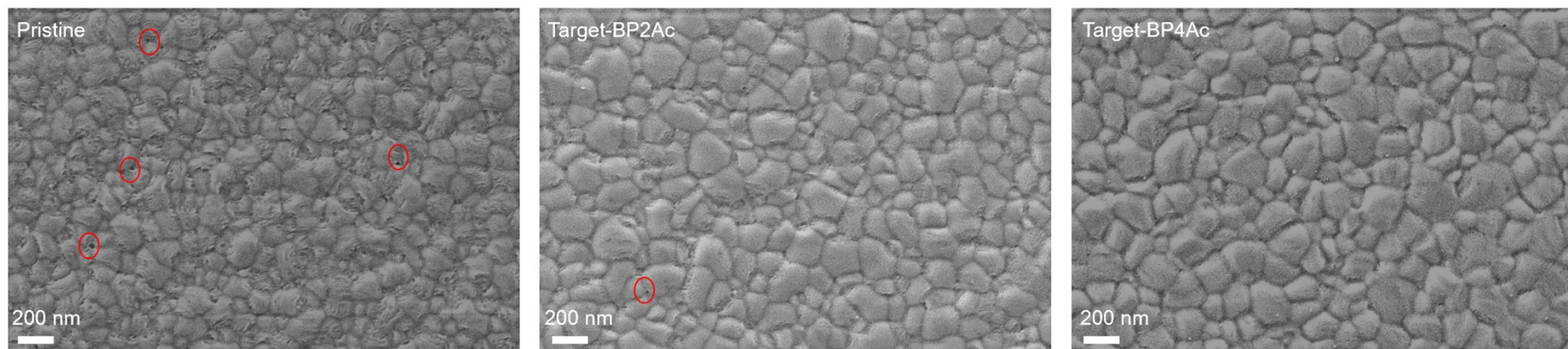
13
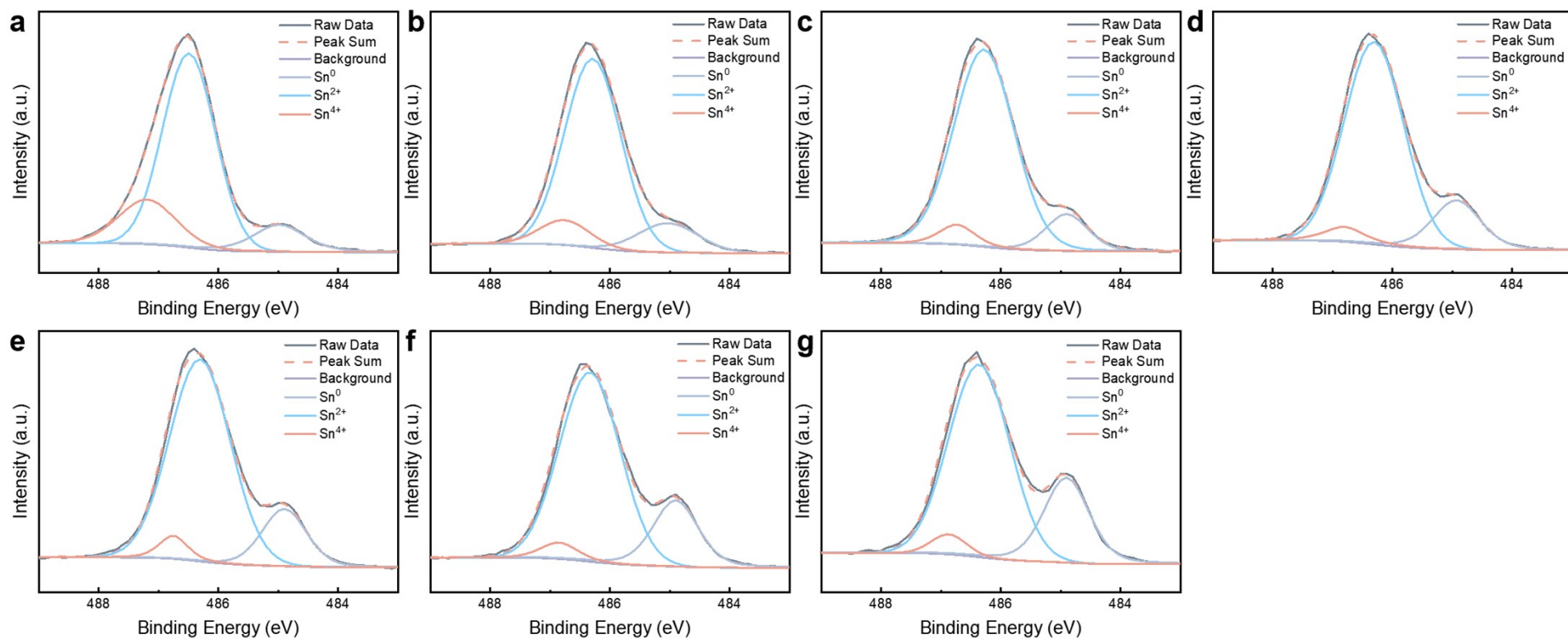
Figure S9. XPS curves of the target-BP4Ac perovskite film at different etching times. The sequence and etching time for this sample are identical with the pristine sample shown in Figure S7.

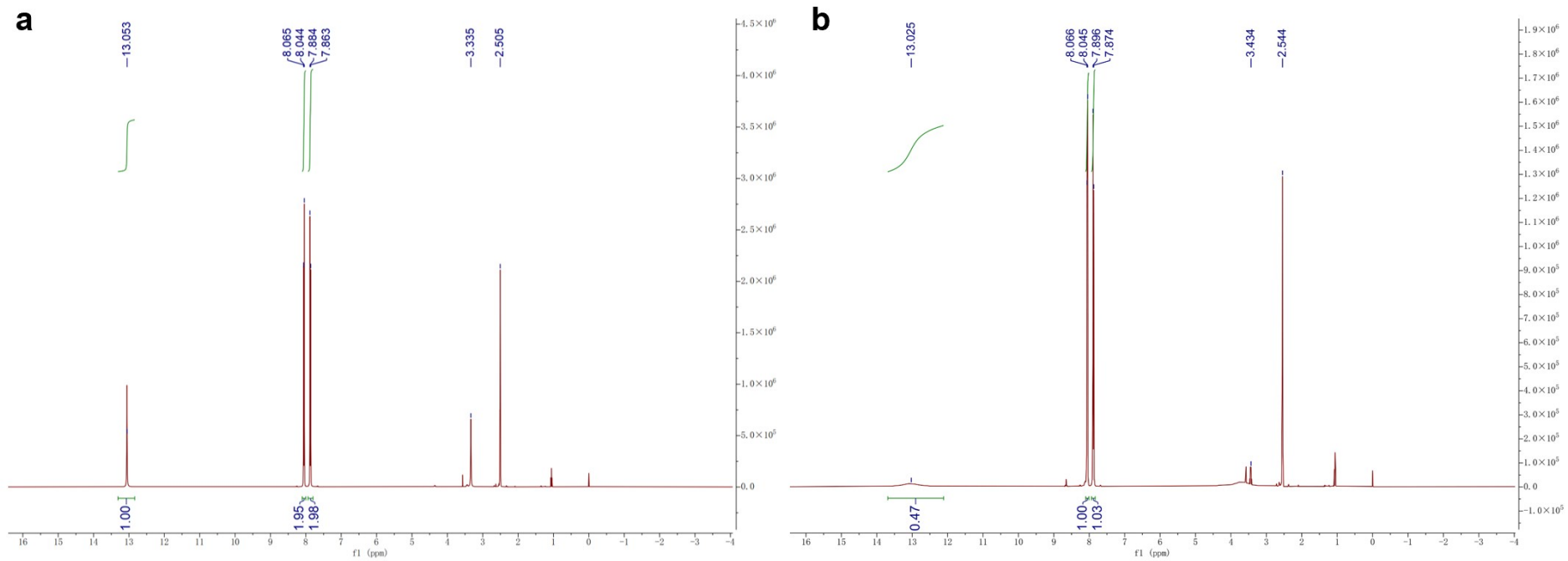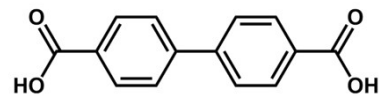**Figure S10.** Top-view SEM images of the perovskite films without and with different additives.

Figure S11. The 1H-NMR results for a) BP2Ac solution and b) BP2Ac + SnI$_2$ solution dissolved in C2D6OS.
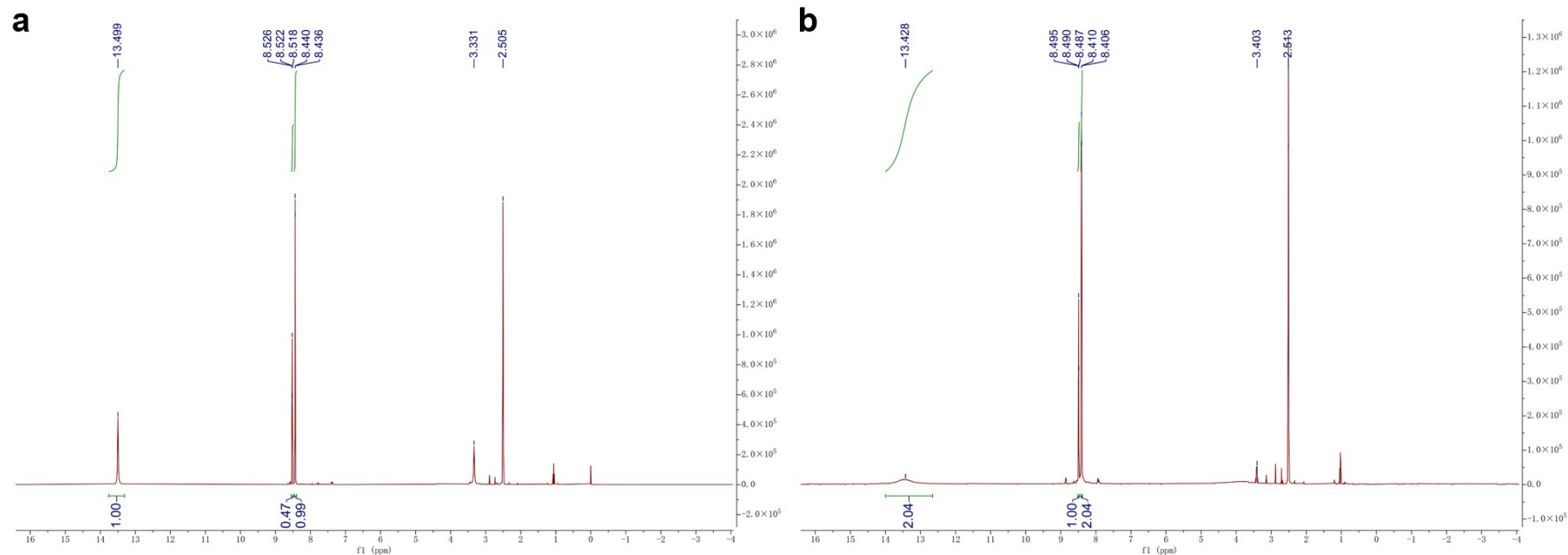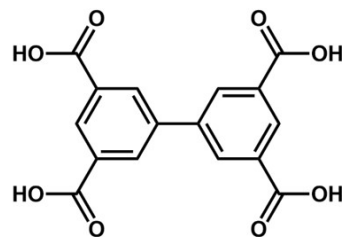
Figure S12. The 1H-NMR results for a) BP4Ac solution and b) BP4Ac + SnI$_2$ solution dissolved in C2D6OS.
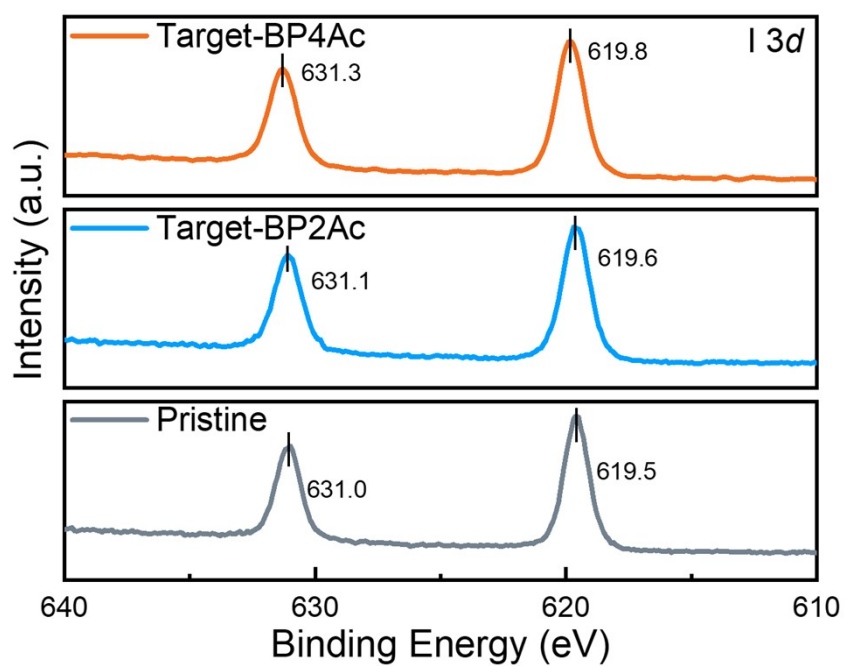
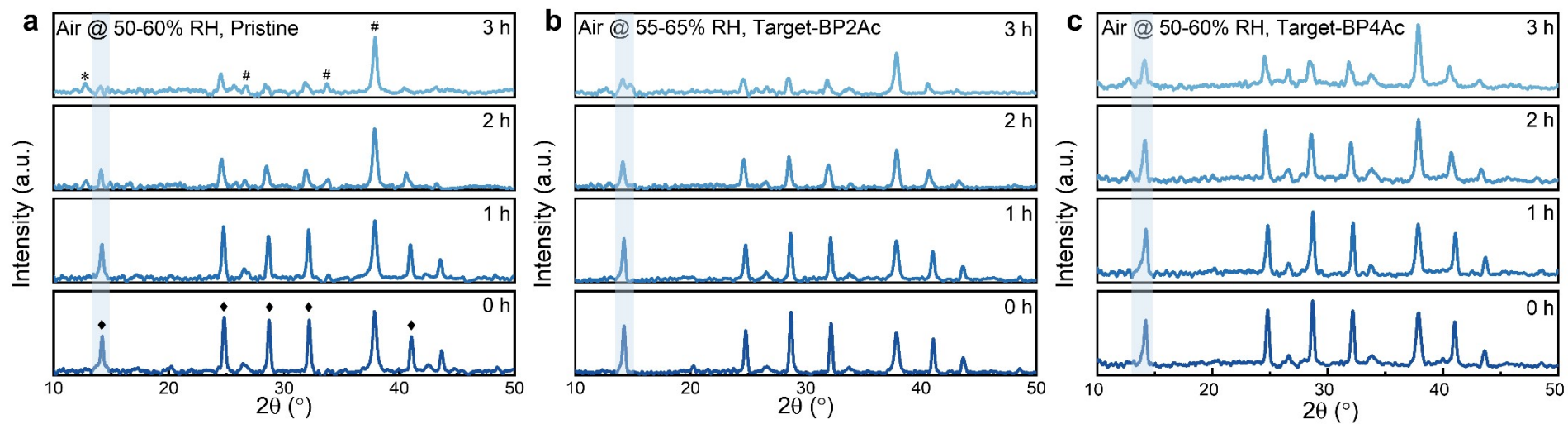**Figure S13.** X-ray photoelectron spectroscopy (XPS) of I 3*d* core levels spectra on the perovskite films.

Figure S14. XRD pattern of perovskite films without or with different additives (# are on behalf of the peaks of FTO, ♦ indicate the diffraction peaks of perovskite and * means diffraction peaks connected with SnI_4).
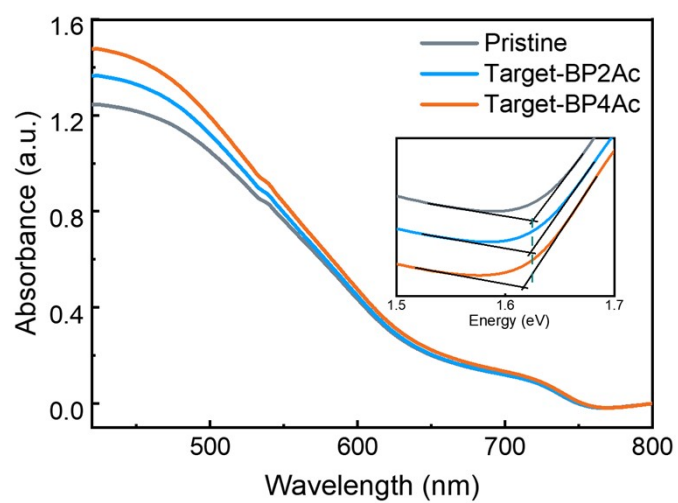
Figure S15. UV-vis absorption spectra and the bandgap (inside) of perovskite films without and with different additives.
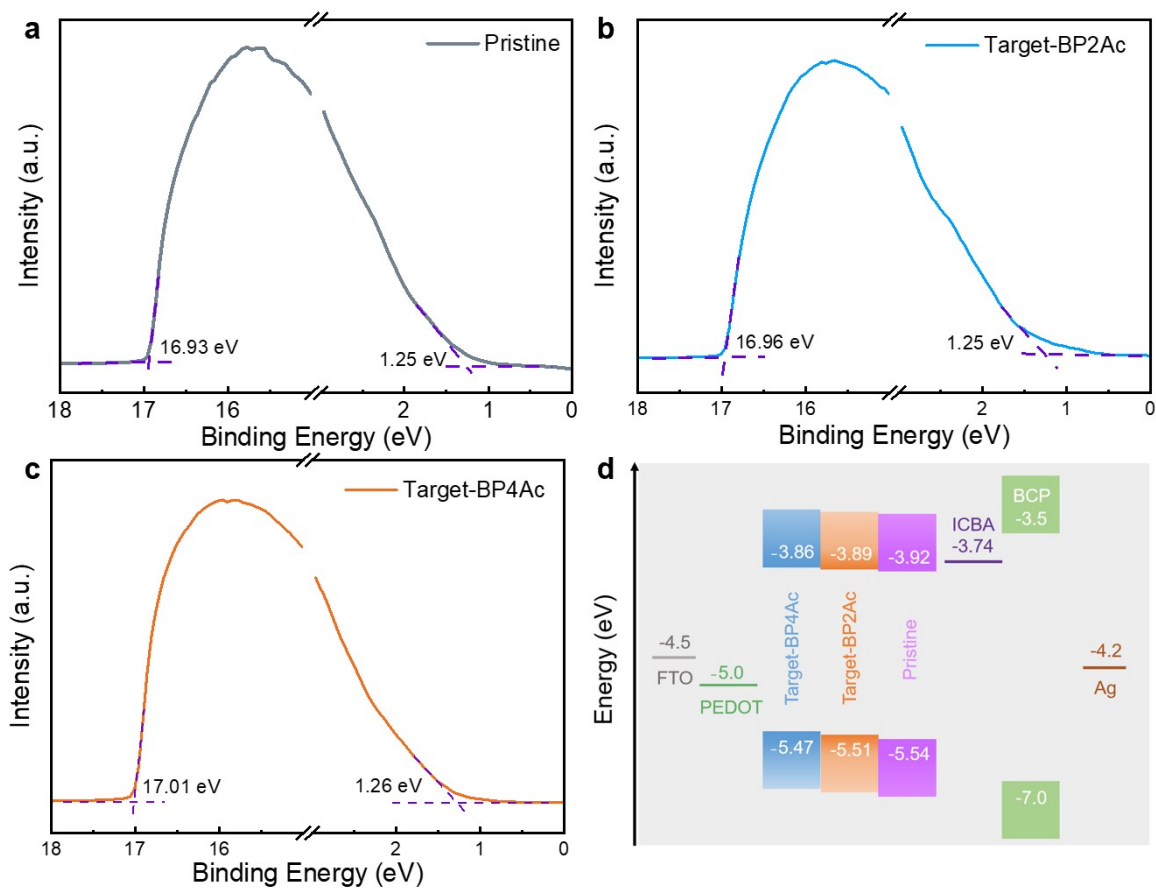
Figure S16. a,b,c) The valence band edges and cutoff regions of UPS spectra, d) The schematic energy-level alignment of Pristine, Target-BP2Ac and Target-BP4Ac films.

Table S1. The pH values of BP2Ac solutions at different concentrations.

Concentration	0 mg/mL	0.5 mg/mL	1 mg/mL	1.5 mg/mL
BP2Ac	5.06	4.62	4.38	3.95

Table S2. Photovoltaic parameters of devices with different concentrations of BP2Ac.

Device	V_{OC} (V)	J_{SC} (mA/cm²)	FF (%)	PCE (%)
Pristine	0.78	14.51	60.7	6.87
0.5 mg/mL	0.85	14.99	69.6	8.87
1.0 mg/mL	0.83	13.65	67.0	7.59
1.5 mg/mL	0.80	13.48	62.7	6.76

Table S3. Photovoltaic parameters of devices with different concentrations of BP4Ac.

Device	V_{OC} (V)	J_{SC} (mA/cm²)	FF (%)	PCE (%)
Pristine	0.78	14.40	60.1	6.75
0.05 mg/mL	0.84	15.09	69.1	8.76
0.1 mg/mL	0.85	16.64	73.2	10.35
0.2 mg/mL	0.80	13. 48	56.0	6.04